Contact Response Maps for Real Time Dynamic Simulation *

C. Ullrich† and D. K. Pai‡
Department of Computer Science and Institute of Applied Mathematics
University of British Columbia
Vancouver, Canada
{ullrich|pai}@cs.ubc.ca

Abstract

We describe the generation and use of "contact response maps" for real time dynamic simulation. Contact response maps are geometry and material dependent maps on physical objects which describe the surface tractions associated with local deformations during contact. We develop a technique for precomputing contact response maps for elastic bodies using the Boundary Element method to solve the corresponding plane strain problem. Such maps can then be used in a real-time simulation environment to accurately resolve collision dynamics.

1 Introduction

Much effort in the past few years has been focused on the simulation of contact and collision phenomena. However, accurate simulation at interactive rates remains challenging. Contact events are extremely fast, and delays in simulating the contact force and motion can lead to instabilities in a control algorithm or destroy the sense of realism in a virtual environment. Unfortunately, the contact response of real objects is very complex; even with somewhat idealized linear viscoelastic models of the materials, simulation requires the numerical solution of partial differential equations (PDEs) on domains with complex shapes. Therefore, much effort has been directed at developing empirical contact models that are sufficiently accurate, while being sufficiently fast for real time simulation.

We present a solution to this problem by introducing a data structure associated with each colliding body called the *contact response map*. The contact response map can produce a more accurate collision response than the rigid body models used in the literature, since it is computed from the governing partial differential equations of the body. On the other hand, the contact response map allows the collision response to be computed rapidly, at rates suitable for control and interactive simulation.

In this paper, we demonstrate this approach with a model of a two dimensional elastic solid, whose behavior is governed by Navier's equation (a system of hyperbolic PDEs). We first show that the response of an elastic solid varies significantly with impact location – this phenomenon is consistent with experimental results (e.g., [SH96]). In addition, we describe an algorithm to make use of the precomputed step response functions in a real time dynamic simulator.

The remainder of the paper is organized as follows: The rest of section 1 discusses related work in the field of impact mechanics. Section 2 discusses the theory of elastic solids subject to impact. Section 3 quickly derives the boundary element method. Section 4 contains the numerical results and relevant notes. Section 5 presents a time stepping algorithm for dynamical simulation. In Section 6 we consider the storage issues for contact maps. Finally in section 7 we summarize the results to date and discuss some possible generalizations of this work.

*Supported in part by grants from NSERC and IRIS.
†M.Sc. student, Mathematics.
‡Associate Professor, Computer Science.

1.1 Related Work

Most models intended for computationally demanding use, including the model in this paper, employ the rigid body assumption. Rigid bodies are idealized physical objects which deform only locally during impacts. Following [Cha97], rigid body impact models may be classified as impulse response rigid or force response rigid.

Impulse response rigid models consider impact events as occurring over an infinitely short period of time, resulting in a discontinuous change in the velocities of colliding bodies. Impulse models define a coefficient of restitution, e, relating post-impact to pre-impact states, quantifying the loss of kinetic energy due to a collision event. The coefficient was defined in terms of change in velocity by Newton, change in normal momentum [Kel86], [Bra89] or the change in normal work [Str90].

It is only recently that consistent algorithms for resolving impulse response rigid collisions were developed. In [WM87], the authors present a complete solution for two dimensional impulsive collision with friction. Three dimensional impulsive collision is complicated by the existence of multiple solutions, as discussed in Bhatt and Koechling [BK95]. A complete 3D impulsive collision algorithm is discussed in [Mir96]. Many other authors present analyses of the 3D impact problem [Bra89, Bar92, PG96]. Chatterjee [Cha97] examined a number of 3D models for energetic consistency and accuracy.

Force response rigid models attempt to model the forces produced during contact. Models in this category typically define a function $f(u, \dot{u})$ that gives force as a function of penetration depth u and velocity $\dot{u}$. Linear force functions are considered in [GPS94a], while more generalized models are discussed in [HF75]. The Hertz model, in which $f(u) \propto u^{\frac{3}{2}}$ can be derived from physical principles as in [Gol60].

Resolving force response rigid collisions is accomplished by enforcing the action-reaction principle (Newton's third law), friction constraints, and the force function. For most models this results in a system of non-linear algebraic equations to be solved at each time step. See [Gol60] or [GPS94a, GPS94b] for detailed algorithms.

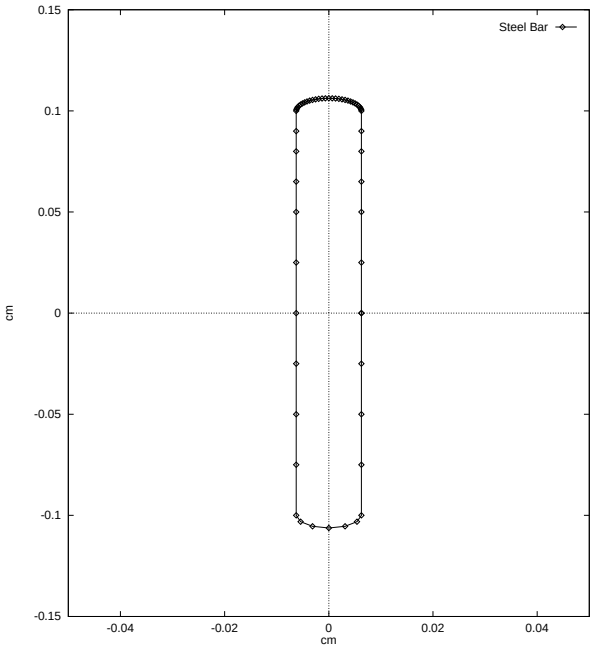

Figure 1: Steel Bar with Boundary Element Nodes shown. 56 nodes are shown, 26 along the bar length, and 28 on the tip. Nodes are more dense near the tip where we apply displacements.

Recent work, especially that of Stoianovici and Hurmuzlu [SH96], has shown the coefficient of restitution to be a geometry dependent phenomenon. In their study, a long thin steel bar (fig. 1) was dropped onto a massive block. The experimental setup allowed the angle of the bar to be varied so that impact occurred at various points around the rounded tip. Their results show the restitution factor varying over a range from .9 for normal impact to as low as .2 for a critical impact angle of about 66 degrees.

All collision models above all try to capture the impact behaviour of an object with a few simple numbers such as the coefficient of restitution, or spring and damping constants (for the linear force law). With the advent of computers that have large memories, we can consider a radically different approach in which we precompute a large number of collision responses for a given object using very accurate, but computationally expensive methods such as finite elements or boundary elements.

2 Theory

2.1 Elastic Approximation and Range of Validity

In this study, we consider only impacts that occur at relatively low velocities. In the case of contact between bodies moving slowly, there will be no permanent deformation at the point of contact, and we are justified in assuming that the solids may be modeled by the elastic constitutive equations.

A recent study by Lim and Stronge [LSar] used finite element calculations to bound the pre-impact velocity in terms of the yield strength of a material. They demonstrated that velocities in the 1-5 m/s range produce no plastic deformation for typical metals such as aluminum or steel.

2.2 Governing Equations

For simplicity we restrict our study to the 2D case. We need to model the response of an elastic solid to a contact event. In 2D, this is most easily done using the equations of plane-strain that model the response of an elastic solid which has negligible variation in the third axis (out of plane).

The field equations (Navier's equation) are written in component form as

$$\mu u_{i,jj} + (\lambda + \mu) u_{j,ji} + \rho b_i = \rho \ddot{u}_i \qquad (1)$$

where $u \in \Omega$, u_i is the i'th component of the displacement, μ and λ are Lamé's constants, b_i is the i'th component of the body force, and ρ is the density. A comma denotes partial differentiation with respect to the space component, $\ddot{u}_i$ is the second time derivative of the i'th component of u. We apply the summation convention to repeated indices. Under the plane strain assumption, the indices i, j in Equation (1) run between 1 and 2. The equation is defined on $\Omega \subset \Re^2$.

2.3 Boundary Conditions

The field equations (1) give the generic behavior of an elastic body, but the boundary conditions specify a particular situation. An elastic body in free space not in contact with any other body has Neumann type boundary conditions. This is because the boundary is free to vibrate much like the free end of a string undergoing wave motion. Thus for all boundary points not in a contact situation (we define this region as Γ_1), we can say:

$$\frac{du}{dn} = 0,$$

where $u \in \Gamma_1$ and n is normal to the boundary Γ_1.

Now for a boundary segment which is in contact with an external body (Γ_2), we specify the displacement explicitly using a Dirichlet condition

$$u \cdot n = d_j,$$

where $u \in \Gamma_2$, and d_j is the j'th displacement depth (see below).

Given the field equations and boundary conditions, we can solve the well posed PDE using a variety of numerical techniques. A popular choice is othe finite element method (FEM) in which the region Ω is discretized to solve the PDE. We consider instead the boundary element method which has a number of advantages over FEM, especially for elastodynamic contact problems.

3 Boundary Element Solution

There has been a great deal of work in the past two or three decades in the boundary element community on the solution of elastostatic and elastodynamic problems. Boundary element (BEM) solution techniques are ideally suited to contact problems because all of the unknowns are on the boundaries of the colliding bodies. In contrast, FEM (finite element) approaches deal with the entire body and solve for stresses and displacements at every point.

The basic idea of BEM is to formulate the partial differential equation as an integral equation. There are several ways of doing this for the Navier field equation. We briefly outline one approach and refer the interested reader to Dominguez [Dom93].

Denote the solution to Eq. 1 by u, with stress field σ and body forces b. Consider a second solution to the field equation (1) — with different initial conditions — for the same geometry, u^* with stress field σ^* and body forces b^*. The weighted residual of the two solutions is written as

$$\int_\Omega (\sigma_{kj,j} * u_k^*) d\Omega + \int_\Omega \rho(b_k * u_k^*) d\Omega - \int_\Omega \rho(\ddot{u}_k * u_k^*) d\Omega = 0, \quad (2)$$

where * denotes a convolution product. Applying the divergence theorem, we can rewrite this as

$$\begin{aligned} &\int_\Gamma (p_k * u_k^*) d\Gamma \\ &+ \int_\Omega \rho(b_k * u_k^* + u_{0k}\dot{u}_k^* + \dot{u}_{0k} u_k^*) d\Omega \\ &= \int_\Gamma (p_k^* * u_k) d\Gamma \\ &+ \int_\Omega \rho(b_k^* * u_k + u_{0k}^* \dot{u}_k + \dot{u}_{0k}^* u_k) d\Omega, \end{aligned} \quad (3)$$

where $u_{0k} = u_k(x, 0)$, $\dot{u}_{0k} = \dot{u}_k(x, 0)$ are initial displacements and velocities respectively. Now, we generate the reciprocal solution u^* as a solution of the field equations when an impulsive load is applied at the point x^i in the direction l, i.e.,

$$\rho b_k^* = \delta(t)\delta(x - x^i)\delta_{lk}. \quad (4)$$

Further, assume the initial conditions are identically zero and that the body forces of the primary solution may be neglected. Then we can write Eq. 3 as

$$u_l(x^i, t) = \int_\Gamma (u_{lk}^* * p_k) - (u_k * p_{lk}^*) d\Gamma, \quad (5)$$

which gives the displacement at point x^i in direction l as a function of the boundary. Note that this same expression can be obtained from a variational principle (see [AP92]).

The integrals in Equation 5 are difficult or impossible to solve analytically. The numerical solution to these integrals constitutes the boundary element method.

Observe that we need only to discretize the boundary, which immediately reduces the dimension of the problem by one. In contrast, the FEM approach requires the domain Ω to be discretized. Typical BEM algorithms divide up the boundary into piecewise constant, linear or quadratic elements. Corners require special treatment. Also, it is not uncommon for the resulting integrals to be highly singular, in which case, the Cauchy principal value is used.

As a result of the discretization of the boundary and approximate evaluation of the integrals, we obtain a system of linear algebraic equations for the unknown boundary displacements or tractions. Although the system is much smaller than a similar FEM system, the matrix presents no special symmetry or sparseness properties and must be solved using dense matrix techniques.

When the integral (5) is discretized, the resulting linear equations can be rearranged so that for nodes on which displacements are given, the tractions are solved for and for nodes with given traction, the displacement is solved for. Hence for our boundary conditions, the BEM gives the surface traction (force response) for the point at which we specify the displacement. We write this as

$$f_j^A(t), \quad (6)$$

which is the contact response at node j for body A. We store a discrete representation of $f_j^A(t)$ at a each boundary node j on a geometric model of body A. This is the contact response map.

4 Numerical Results

We considered a metal bar with the same dimensions as in [SH96], 20 cm in length with a diameter of 12.5mm and spherical ends (see fig. 1). The boundary was discretized using 28 quadratic boundary elements, with three node points each. Using software developed by Dominguez [Dom93] for the simulation of elastodynamic systems, we computed the traction response at a number of node points to a step displacement. Calculations were performed on a Pentium II 266MHz computer, with each curve taking 3-4 minutes to generate. The results are

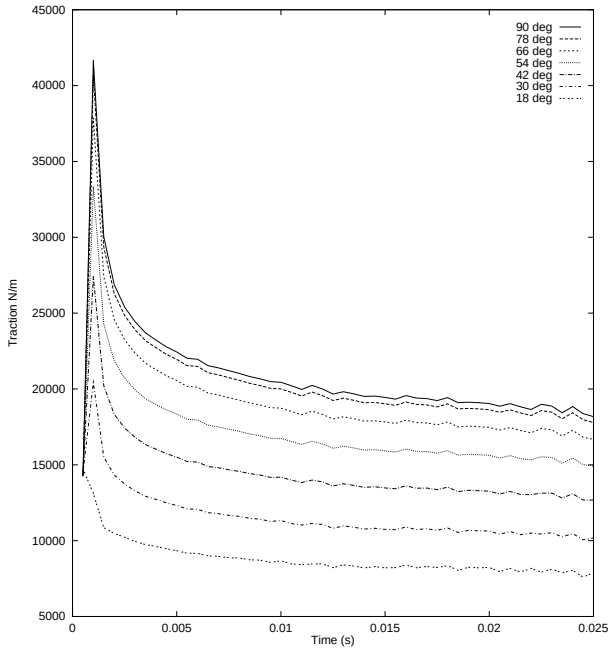

Figure 2: Step response curves for various impact angles at bar end. Angles are measured with respect to the horizontal axis of the bar in Figure 1.

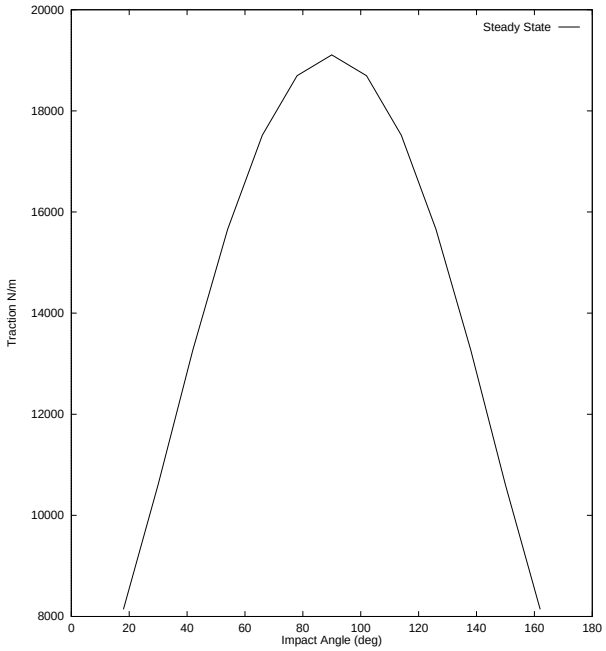

Figure 3: Steady state tractions giving the spring constant for each impact angle.

shown in fig. 2 and clearly demonstrate the dependence on geometry of impact location.

The traction response curves shown in fig. 2 can be utilized for dynamic simulation in a variety of ways. Because we use a linear elastic model, the traction due to an arbitrary displacement trajectory $u(t)$ can be reconstructed from the contact response map by the superposition principle. We describe this in §5.

One could also use the contact response map to estimate parameters for simpler contact models. For instance, consider the steady state response calculated from the tail end of the step response using an average (constant fit). In using only the steady state, we are effectively generating the proportionality ("spring") constant k in a force response rigid law $f(y) = -ky$. This law is only intended to demonstrate the simplest application of these results. Nevertheless, even this approximation demonstrates the geometry dependence of the contact response. This can be seen in Figure 3, which plots the effective spring constant k with respect to the contact position (angle) on the bar tip.

More complex force models can be fit to BEM data by modifying the displacement function. In our examples we use a step function, but suppose we wanted to generate coefficients for a model such as $f(u, \dot{u}) = -au^{\frac{3}{2}}$. One approach would be to calculate the force response for a linear displacement $u(t) = t$, and then fit the given function to the resulting curve. Though such a fit may in fact be a poor approximation (since we have a linear elastic solid), it will still incorporate a geometric dependence, where previously there was none. The suitability of particular models is discussed in detail in [HF75].

5 Contact Simulation

We now develop an algorithm which uses the precomputed boundary element surface tractions to generate collision forces during interactive simulations.

5.1 Action Reaction

The remaining requirement for a full solution to the contact problem is to enforce the action-reaction principle, or Newton's Third Law. As this is dependent on the exact contact configuration, it must be done during the simulation process. We state this requirement as: $f^A = -f^B$.

In our model, the response of the elastic solid is linear in the displacement depth, which allows us to write the force as a function of current depth and any residual effects from previous depths.

To simulate the contact, it is possible to define several numerical schemes for time stepping. We outline one scheme here; for simplicity we present the frictionless case — since the algorithm computes the normal contact force, one can extend this method to include Coulomb friction effects, as in [GPS94a].

We first introduce some additional notation. Let the nominal, undeformed position of the contact point on body A be $\tilde{u}^A$, and let the actual position be u^A; then the penetration of A, δ^A, is defined as

$$\delta^A = \tilde{u}^A - u^A.$$

When the time needs to be specified, we will use the abbreviation $\delta^A_k = \delta^A(t_k)$ and the backward time difference operator Δ, defined as

$$\Delta\delta^A_k = \delta^A_k - \delta^A_{k-1}.$$

Finally, let $f_s(t)$ be the surface traction response to a unit step (of boundary node displacement) at $t = 0$.

At time t_k, we advance the simulation to time t_{k+1} as follows:

1. Compute the nominal forces on the body due to penetration upto time t_k.

   $$\tilde{f}^A_{k+1} = \sum_{j=0}^{l} f^A_s(t_{k+1} - t_{k-j})\Delta\delta^A_{k-j}.$$

   $\tilde{f}^B_{k+1}$ is computed similarly. We note that if the time steps are of equal size, this is can be done efficiently as a digital filter applied to the penetration trajectory.

2. Integrate the equations of motion for each body (which may be part of a larger multibody system), using an appropriate ODE or DAE integrator, and compute the nominal positions $\tilde{u}^A_{k+1}$ and $\tilde{u}^B_{k+1}$. Integration of multibody dynamics equations is treated extensively elsewhere in the literature (e.g., [APC97]).

3. Compute the total penetration along the contact surface normal n as

   $$\delta_{k+1} = (\tilde{u}^A_{k+1} - \tilde{u}^B_{k+1}) \cdot n^B.$$

   Here n is pointed from B to A. We assume that the the total displacement of the bodies during contact is small relative to spacing of boundary element nodes.

4. Action-Reaction. Compute the penetration of each body so that it satisfies the kinematic constraint

   $$\delta^A_{k+1} + \delta^B_{k+1} = \delta_{k+1} \tag{7}$$

   and Newton's third law

   $$f^A_{k+1} = -f^B_{k+1}. \tag{8}$$

   Since

   $$f^A_{k+1} = \tilde{f}^A_{k+1} + f^A_s(t_{k+1} - t_k)\Delta\delta^A_k,$$

   this is a linear equation in δ^A_{k+1} and δ^B_{k+1}. Therefore we can solve the Equations 7 and 8 simulataneously for the actual penetrations δ^A_{k+1} and δ^B_{k+1}.

   If necessary, f^A_{k+1} and u^A_{k+1} can be computed from δ^A_{k+1}.

5. Advance time to t_{k+1}.

5.2 Sustained Contact, Multiple Contacts

Since the model we describe is force response rigid, sustained contact requires no special processing. This is a definite advantage over impulsive models which require additional calculations and assumptions to handle long term contact situations.

Force response models also have the advantage that multiple contacts are handled simply by superposition. In the impulse case, multiple contacts are known to cause (sometimes severe) uniqueness problems as discussed in [Bar92].

6 Storage considerations

Clearly this approach to dynamic simulation uses more memory per object than the coefficient of restitution approach [Cha97] or the spring-damper approach [GPS94a]. For each boundary element, we store N_f numbers to describe the force response ($N_f = 1$ for our steady state model). We can write the total storage per object as $N_b N_f$ floating point numbers. However, this is modest by the standards of today's computers. For example, in our study $N_f = 1$ and we used $N_b = 28$ boundary elements. Even to store the full force response we need at most $N_f = 100$, and the number of boundary points can often be reduced by considering object symmetries.

7 Conclusions

We presented a numerical technique to quantitatively generate force response, given a geometry and material parameters. Our approach is more accurate than impact laws currently used for real time simulation, since it is based the PDEs of linear elastic solids. The PDEs are solved using well established boundary element method. Our approach captures experimentally observed impact phenomena such as the dependence of the contact response on the particular geometry of impacting objects. Given a computed force response, real time simulation becomes a possibility even for complex multibody systems. This will allow for the construction detailed virtual environments that can be relied upon as faithful representations of the real world, useful for engineering, education and countless other fields.

In future work, we plan to extend this approach to other types of continuous media such as viscoelastic and anisotropic materials, and to demonstrate it in a 3D simulation enviornment being developed in our lab. We also plan to directly estimate the contact response map for more complex objects, from responses measured with our ACME facility.

References

[AP92] H. Antes and P. D. Panagiotopoulos. *The Boundary Integral Approach to Static and Dynamic Contact Problems.* Birkhauser, Basel - Boston - Berlin., 1992.

[APC97] U. Ascher, D. K. Pai, and B. Cloutier. Forward dynamics, elimination methods, and formulation stiffness in robot simulation. International Journal of Robotics Research, 16:6, December 1997. (to appear).

[Bar92] D. Baraff. *Dynamic Simulation of Non-Penetrating Rigid Bodies.* PhD thesis, Cornell University, 1992.

[BK95] V. Bhatt and J. Koechling. Three-dimensional frictional rigid-body impact. *ASME Journal of Applied Mechanics*, 62:893–898, 1995.

[Bra89] R. M. Brach. Rigid body collisions. *ASME Journal of Appied Mechanics*, 56:133–138, 1989.

[Cha97] A. Chatterjee. *Rigid Body Collisions: Some General Considerations, New Collision Laws, and Some Experimental Data.* PhD thesis, Cornell University, 1997.

[Dom93] J. Dominguez. *Boundary Elements in Dynamics.* Elsevier Science, Essex, 1993.

[Gol60] W. Goldsmith. *Impact: The theory and physical behavior of colliding solids.* Edward Arnold, London, 1960.

[GPS94a] S. Goyal, E. Pinson, and F. Sinden. Simulation of dynamics of interacting rigid bodies including friction i: General problem and contact model. *Engineering with Computers*, 10:162–174, 1994.

[GPS94b] S. Goyal, E. Pinson, and F. Sinden. Simulation of dynamics of interacting rigid bodies including friction ii: Software system design and implementation. *Engineering with Computers*, 10:175–195, 1994.

[HF75] K. H. Hunt and Crossley F.R.E. Coefficient of restitution interpreted as damping in vibroimpact. *ASME Journal of Applied Mechanics*, 42:440–445, 1975.

[Kel86] J. B. Keller. Impact with friction. *ASME Journal of Applied Mechanics*, 53:1–4, 1986.

[LSar] C. T. Lim and W. J. Stronge. Normal elastic-plastic impact in plane strain. *Math and Computer Modeling*, to appear.

[Mir96] B. Mirtich. *Impulse-based Dynamic Simulation of Rigid Body Systems*. PhD thesis, UC Berkeley, 1996.

[PG96] F Pfeiffer and C Glocker. *Multibody Dynamics with Unilateral Contacts*. Wiley, New York, 1996.

[SH96] D. Stoianovici and Y. Hurmuzlu. A critical study of the applicability of rigid-body collision theory. *ASME Journal of Applied Mechanics*, 63:307–316, 1996.

[Str90] W. J. Stronge. Rigid body collisions with friction. *Proc. R. Soc. Lond. A*, 431:169–181, 1990.

[WM87] Y. Wang and M. Mason. Modeling impact dynamics for robotic operations. In *IEEE International Conference on Robotics and Automation*, pages 678–685, 1987.